Academic Journal of Applied Sciences
ISSN: 3105-0549 (Print), ISSN: 3105-0557 (Online) | Vol. 1, No. 2, 2026

Calcium Alginate Hydrogel Filtration Membrane Reinforced by Vacuum Drying and Its Separation Performance for Dye

Wei Zhang [1, 2], Jiabao Cui [1, 2], Kongyin Zhao [1, *], Xiaoyin Wang [1]

[1] State Key Laboratory of Advanced Separation Membrane Materials, Tianjin 300387, PR China

[2] School of Materials Science and Engineering, Tiangong University, Tianjin, 300387, PR China

[*] **Corresponding author**: (Email: tjzhaokongyin@163.com)

Abstract: Calcium alginate (CaAlg) hydrogel membranes have demonstrated great application potential in the separation field owing to their excellent antifouling properties, yet their inherent insufficient mechanical strength has severely restricted their large-scale applications. To address this issue, in this study, CaAlg hydrogel membranes were prepared via the ion crosslinking method, and a vacuum drying-rehydration process was adopted for post-treatment, achieving the goal of reinforcing the membrane's mechanical properties while preserving its separation efficiency. Low-field nuclear magnetic resonance (LF-NMR) analysis revealed that free water and bound water inside the membrane were gradually lost during the drying process, and this change was directly correlated with the reduction of membrane thickness and the improvement of tensile strength. Performance test results showed that the optimized membrane exhibited stable rejection performance against various dye pollutants under low-salt conditions, with a rejection rate higher than 95% and a water permeation flux ranging from 8.5~17.5 $L \cdot m^{-2} \cdot h^{-1}$. The flux was jointly affected by the operating pressure and the molecular weight of the dye. This study revealed the balancing mechanism between mechanical reinforcement and separation performance of CaAlg hydrogel membranes, providing new insights and technical support for the development of sustainable membrane materials in the fields of wastewater treatment and carbon capture.

Keywords: Calcium alginate hydrogel, Vacuum drying, Dye filtration, Mechanical properties, Filtration membrane.

1. Introduction

The textile and dyeing industry is one of the major sources of global industrial wastewater. However, the wastewater discharged from its production process is characterized by large water volume, high chroma, high COD concentration, complex composition, poor biodegradability, and high salinity, which has become a key challenge and research focus in industrial wastewater treatment [1-3]. Traditional processes such as biological treatment, flocculation and sedimentation, and activated carbon adsorption exhibit limited removal efficiency for structurally stable synthetic dyes, and can hardly meet the increasingly stringent discharge standards and the demand for reclaimed water reuse [4, 5]. Membrane separation technology, with the advantages of efficient decolorization and precise separation of dyes and salts, has shown broad application prospects in the advanced treatment of dyeing wastewater [6-8].

Sodium alginate hydrogel membranes, which possess excellent hydrophilicity, biocompatibility, and efficient adsorption and rejection capacity for dye molecules, are recognized as a green and efficient novel separation membrane material [9, 10]. However, pure CaAlg hydrogel membranes generally suffer from problems such as low mechanical strength, easy swelling in aqueous environments, and poor structural stability. In practical dyeing wastewater treatment, this leads to phenomena including membrane deformation, uncontrolled pore size, reduced rejection efficiency, and flux decay, which severely restricts their engineering application [11, 12]. Therefore, the development of modified CaAlg hydrogel membranes with both high separation performance and good structural stability has important theoretical significance and application value for improving the efficiency of dyeing wastewater treatment and promoting the green and sustainable development of the textile industry [13, 14].

To address this issue, the drying-rehydration post-treatment process has been proposed to assist in improving the mechanical strength and structural stability of hydrogels [15, 16]. Existing studies have shown that after drying and rehydration treatment, CaAlg hydrogels can achieve improved mechanical strength through the strengthening of intermolecular forces and the densification of the crosslinking network: during the drying process, the internal moisture of the hydrogel volatilizes, the intermolecular distance is shortened, and hydrophilic groups such as carboxyl and hydroxyl groups form more hydrogen bonds and intermolecular forces. Meanwhile, the original calcium ion crosslinking bonds are further densified, constructing a more stable three-dimensional network structure. In the rehydration stage, the densified network can effectively limit the excessive swelling of the hydrogel, reduce the leaching of calcium ions, retain the reinforced structure formed during the drying process, and thus improve the tensile strength and toughness of the membrane [17, 18]. Ji et al. [11] experimentally verified the enhancement effect of this process on the mechanical properties of CaAlg hydrogels, and found that it can significantly densify the calcium ion crosslinking network and reduce swelling deformation. However, most of these studies adopted the freeze-drying method. Although it can preserve the porous structure of the membrane, leading to more significant improvement of mechanical strength after rehydration and less prone to brittle fracture, the equipment cost is high, which can hardly meet

the demand for large-scale application [19].

To develop a low-cost modification process, this study adopted the vacuum drying process for the post-treatment of CaAlg hydrogel membranes. Compared with traditional hot-air drying, vacuum drying reduces the environmental pressure to enable the rapid volatilization of moisture at a lower temperature, eliminating the need for high-temperature heating. This can avoid the damage to the membrane structure caused by high temperature, and meanwhile, the uniform volatilization rate of moisture can reduce membrane shrinkage and crack generation, promote the formation of intermolecular hydrogen bonds and the densification of the crosslinking network, making it more suitable for the post-treatment requirements of CaAlg hydrogel filtration membranes [13]. This conclusion is consistent with the research results of Xu et al. [19], who found that mild drying methods can effectively preserve the crosslinking structure of hydrogels and avoid the strength degradation caused by calcium ion leaching.

This study systematically investigated the influence law of vacuum drying time on the internal water state, mechanical properties, and separation performance of CaAlg hydrogel membranes, optimized the preparation process parameters, and verified the application performance of the membrane in the fields of dye filtration and dye separation. This provides a theoretical basis and technical support for the development of high-performance, sustainable alginate-based separation membranes.

2. Experimental Section

2.1. Experimental Materials and Instruments

Experimental Materials: Sodium alginate (NaAlg), Calcium chloride ($CaCl_2$), Direct Black (DB), Methyl Orange (MO), Coomassie Brilliant Blue (CBB), and Sodium chloride (NaCl) were all purchased from Shanghai Aladdin Biochemical Technology Co., Ltd., analytical grade. Deionized water was used as the experimental water.

Experimental Instruments: Magnetic stirrer, Vacuum drying oven, Refrigerator, Electronic balance, Thermogravimetric-differential thermal analyzer (TG-DTG), Fourier transform infrared spectrometer (FT-IR), Low-field nuclear magnetic resonance analyzer (LF-NMR), Universal testing machine, Membrane separation performance testing device.

2.2. Preparation of CaAlg Hydrogel Filtration Membrane

A NaAlg solution with a mass fraction of 2.5% was prepared, which was magnetically stirred at room temperature for 3 h until sodium alginate was completely dissolved, obtaining a uniform and stable casting solution. The casting solution was placed in a vacuum drying oven to remove air bubbles, and then refrigerated in a refrigerator for 12 h to fully stabilize the casting solution system.

A glass rod wrapped with copper wires of 0.5 mm diameter was used to control the thickness of the wet membrane, and the casting solution was uniformly scraped onto the surface of a clean glass plate to ensure that the scraped coating had uniform thickness, without bubbles or scratches. Subsequently, the glass plate was immersed into a $CaCl_2$ solution with a mass fraction of 2.5% for ion crosslinking. After the casting solution was completely gelled, the CaAlg hydrogel membrane was obtained. The prepared membrane was sealed and immersed in 2.5 wt.% $CaCl_2$ solution for storage, to prevent membrane swelling and structural loosening caused by calcium ion leaching.

2.3. Drying-Rehydration Post-Treatment Process

The CaAlg hydrogel membranes were taken out of the $CaCl_2$ solution, rinsed to remove the residual solution on the surface, and then placed in a vacuum drying oven. Under the conditions of room temperature and a vacuum degree of 0.08 MPa, the membranes were dried for 0 min (undried), 20 min, 40 min, and 60 min respectively, to prepare membrane samples with different drying durations. The dried membranes were immersed in deionized water for rehydration treatment, until the membranes reached swelling equilibrium, for subsequent characterization and performance tests.

2.4. Characterization and Performance Tests

(1) Thermogravimetric-differential thermal analysis (TG-DTG): The thermogravimetric- differential thermal analyzer was used to determine the thermal decomposition behavior of NaAlg and CaAlg hydrogel membranes and analyze their thermal stability, under a nitrogen atmosphere, with a heating rate of 10 ℃/min and a temperature range from room temperature to 600 ℃.

(2) Fourier transform infrared spectroscopy (FT-IR): The Fourier transform infrared spectrometer was used to analyze the changes of functional groups of NaAlg and CaAlg hydrogel membranes and verify the occurrence of the ion crosslinking reaction, with a test range of 400~4000 cm^{-1}.

(3) Low-field nuclear magnetic resonance (LF-NMR): The low-field nuclear magnetic resonance analyzer was used to determine the transverse relaxation time (T2) of CaAlg hydrogel membranes with different drying times and after rehydration, and analyze the existing state and migration law of the internal water inside the membrane.

(4) Mechanical property test: The universal testing machine was used to determine the tensile strength and elongation at break of CaAlg hydrogel membranes with different drying times and after rehydration, in accordance with the GB/T 1040.3-2006 standard. Each sample was tested 3 times, and the average value was taken.

(5) Membrane separation performance test: The membrane separation performance testing device was used, with dye solutions of different concentrations and dye-NaCl mixed solutions as the feed solution, to explore the effects of operating pressure, drying time, and dye concentration on the water permeation flux and dye rejection rate of the membrane. Meanwhile, the separation ability of the membrane for dyes and NaCl was analyzed.

3. Results and Discussion

3.1. Thermal Stability and Chemical Structure Characterization of CaAlg Hydrogel Filtration Membrane

As can be seen from the macroscopic morphology photo of Figure 1(a), the CaAlg hydrogel membrane after 60 min of drying was milky white and translucent, with a brittle and fragile texture. Obvious shrinkage marks and fine cracks existed on the surface, irregular damage appeared at the edge, and the flexibility was extremely poor, with only no obvious wrinkles generated. This macroscopic morphology feature is

consistent with the results of the mechanical property test, which showed that after 60 min of drying, the membrane material was embrittled and the elongation at break decreased significantly.

The internal mechanism is as follows: excessive drying removes a large amount of internal water of the membrane, greatly reduces the intermolecular chain distance, and leads to excessive densification of the crosslinking network, which eventually causes the membrane material to lose elasticity, become brittle and harden. At the same time, the internal stress generated by the uneven shrinkage of the membrane during the drying process is the core reason for the induction of surface cracks, edge damage, and the slight decrease of tensile strength. The above results indicate that although vacuum drying can effectively inhibit the severe wrinkle deformation of the membrane, excessive drying can still significantly damage the structural integrity of the membrane material, making it unable to meet the structural stability requirements of anti-water flow impact and pressure-bearing operation under the working conditions of dyeing wastewater treatment.

Figure 1(b) shows the SEM image (×5000) of the completely dried CaAlg hydrogel membrane. It can be seen that the membrane surface presents a dense porous structure, with pore collapse and aggregation phenomenon in some regions, and obvious microcracks and concave-convex protrusions on the surface. Compared with the membrane dried for 40 min, the pore size of the completely dried membrane was significantly reduced, the number of pores was decreased, and the compactness was further improved.

This is because during the excessive drying process, the free water and part of the bound water inside the membrane are completely removed, the intermolecular hydrogen bonding effect is excessively enhanced, leading to excessive shrinkage of the crosslinking network, and the pores are squeezed and collapsed. While the surface microcracks originate from the unreleasable internal stress generated by the uneven shrinkage of the membrane during the drying process. The existence of microcracks will further weaken the mechanical strength of the membrane, causing the membrane to be easily damaged. In addition, the dense and non-uniform pore structure will hinder the mass transfer process of water molecules and dye molecules, which is the core reason for the significant decrease of water permeation flux of the membrane dried for 60 min, echoing the subsequent results of the membrane separation performance test.

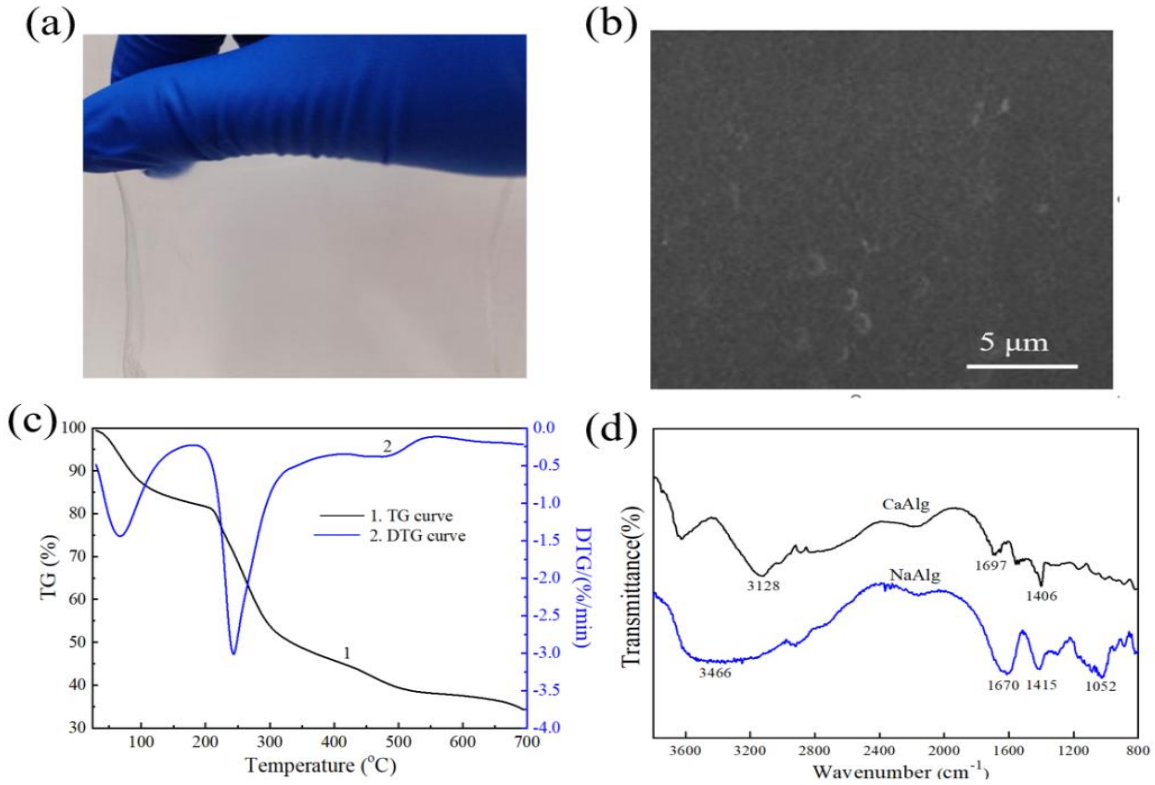

Figure 1. (a) Digital photo of CaAlg hydrogel membrane after 60 min of drying; (b) Scanning electron microscope (SEM) image of completely dried CaAlg hydrogel membrane; (c) TG-DTG curves of NaAlg and CaAlg hydrogel membranes; (d) FT-IR spectra of NaAlg and CaAlg hydrogel membranes

Figure 1(c) shows the TG-DTG curves and FT-IR spectra of NaAlg and CaAlg hydrogel membranes. It can be seen from the TG curves that the thermal decomposition processes of both NaAlg and CaAlg hydrogel membranes are divided into three stages: The first stage (room temperature ~ 150 ℃) is the water evaporation stage, which is mainly the volatilization of adsorbed water and bound water inside the membrane, and the mass loss in this stage is mainly due to water loss. The second stage (150~350 ℃) is the macromolecular chain degradation stage, the molecular chains of NaAlg and CaAlg are broken and degraded, with a relatively fast mass loss rate. The third stage (350~600 ℃) is the carbonization stage of residual substances, the degradation products are further carbonized, and the mass loss tends to be gentle. By comparison, the initial degradation temperature of the CaAlg hydrogel membrane (about 200 ℃) is higher than that of NaAlg (about 180 ℃), and the mass residual rate at the same temperature is higher, indicating that the ion crosslinking effect between calcium ions and alginate anions enhances the stability of the molecular chains, and improves the thermal stability of the CaAlg hydrogel membrane. This is consistent with the result that the maximum thermal decomposition rate peak of CaAlg in the DTG curve shifts to the high temperature direction.

It can be seen from the FT-IR spectrum of Figure 1(d) that, for NaAlg, there is a stretching vibration peak of hydroxyl group (-OH) at 3466 cm^{-1}, and asymmetric and symmetric stretching vibration peaks of carboxyl group (-COO-) at 1670 cm^{-1} and 1415 cm^{-1} respectively. For the CaAlg hydrogel membrane, the -OH stretching vibration peak (3466 cm^{-1}) is weakened and shifts to a lower wavenumber. The asymmetric stretching vibration peak of -COO- (1670 cm^{-1}) shifts to 1697 cm^{-1}, and the symmetric stretching vibration peak (1415 cm^{-1}) shifts to 1406 cm^{-1}. Meanwhile, a new characteristic peak appears at 1052 cm^{-1}, which is the characteristic peak of the coordination bond formed between calcium ions and -COO-. This indicates that an effective ion crosslinking reaction occurred between NaAlg and $CaCl_2$, and the CaAlg hydrogel membrane was successfully prepared.

3.2. Effect of Drying Time on The Water State of Caalg Hydrogel Membranes

Figure 2 shows the LF-NMR T2 spectra and water content change curves of CaAlg hydrogel membranes with different drying times and after rehydration. In LF-NMR, the T2 value reflects the binding state of water inside the membrane. The smaller the T2 value, the tighter the binding between water and the membrane matrix; the larger the T2 value, the easier the water migration. It can be seen from Figure 2(a) that the undried CaAlg hydrogel membrane has two obvious T2 peaks, which correspond to free water (T2≈100 ms) and bound water (T2≈10 ms) respectively. Among them, the peak intensity of free water is relatively high, indicating that there is a large amount of freely migratable water inside the undried membrane, and the network structure is loose.

With the extension of drying time, the peak intensity of free water gradually decreases, the peak intensity of bound water gradually increases, and the T2 value gradually decreases. When the drying time reaches 40 min, the free water peak basically disappears, and only the bound water peak exists, indicating that during the drying process, a large amount of free water inside the membrane is removed, the intermolecular distance is shortened, hydrophilic groups such as hydroxyl and carboxyl groups form more hydrogen bonds, and the binding between water molecules and the membrane matrix is tighter.

After rehydration, a weak free water peak appears in the T2 spectrum of the membrane, but the peak intensity is much lower than that of the undried membrane, and the bound water peak still dominates, indicating that the drying-rehydration process can make the membrane form a denser network structure, limit the entry and migration of water, and reduce the swelling deformation of the membrane. It can be seen from Figure 2(b) that with the extension of drying time, the water content of the membrane gradually decreases, and the water content tends to be stable after 40 min of drying. After rehydration, the water content of the membrane recovers to a certain extent, but it is still lower than that of the undried membrane, which further confirms that the drying-rehydration process can densify the network structure of the membrane and improve its anti-swelling ability.

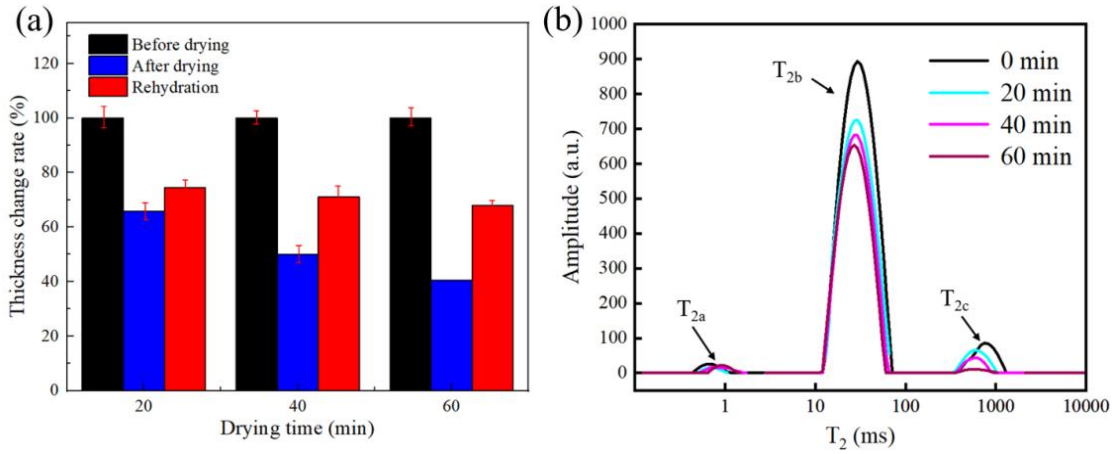

Figure 2. (a) LF-NMR T2 spectra of CaAlg hydrogel membranes with different drying times and after rehydration; (b) Water content change curves of CaAlg hydrogel membranes with different drying times and after rehydration

3.3. Effect of Drying Time on the Mechanical Properties of CaAlg Hydrogel Membranes

Figure 3 shows the tensile strength and elongation at break curves of CaAlg hydrogel membranes with different drying times and after rehydration. It can be seen from Figure 3(a) and (b) that the undried CaAlg hydrogel membrane has a low tensile strength (about 1.10 MPa) and a high elongation at break, indicating that it has weak mechanical strength, good toughness, but loose structure and easy deformation.

With the extension of drying time, the tensile strength of the membrane gradually increases, and the elongation at break gradually decreases. When the drying time is 40 min, the tensile strength reaches the maximum value (about 1.60 MPa), which is about 45.5% higher than that of the undried membrane. When the drying time is further extended to 60 min, the tensile strength decreases slightly, the elongation at break further decreases, and embrittlement phenomenon appears.

As shown in Figure 3(c) and Figure 3(d), the elastic modulus and fracture energy of the dried CaAlg hydrogel membrane and the rehydrated CaAlg hydrogel membrane are both higher than those of the undried CaAlg hydrogel membrane, indicating that the rehydration process can effectively retain the reinforced structure formed during the drying process, and improve the mechanical properties of the CaAlg hydrogel membrane. After rehydration, the tensile strength of the membranes with different drying times all decrease slightly, but they are still higher than that of the undried membrane. Among them, the tensile strength of the membrane rehydrated after 40 min of drying is still maintained above 1.50 MPa, with good toughness and no obvious embrittlement phenomenon.

This is because during the drying process, the internal

water of the membrane volatilizes, the calcium ion crosslinking network is further densified, and the intermolecular hydrogen bonding effect is enhanced, thereby improving the mechanical strength. But excessive drying will lead to the embrittlement of the membrane, and it is difficult to fully recover the elasticity after rehydration, leading to the decrease of tensile strength. Therefore, the appropriate drying time (40 min) can significantly improve the mechanical strength of the CaAlg hydrogel membrane through the drying-rehydration process, while retaining good toughness, to meet the actual operation requirements of dyeing wastewater treatment.

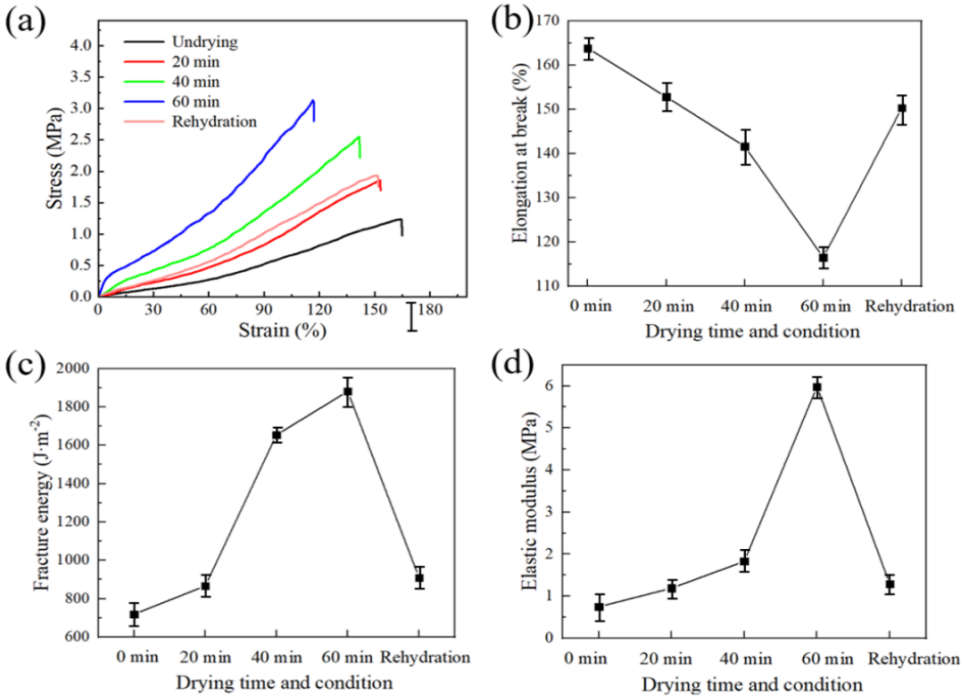

Figure 3. Mechanical property curves of CaAlg hydrogel membranes with different drying times and after rehydration

3.4. Effect of Operating Pressure on the Membrane Separation Performance

Figure 4 shows the change curves of water permeation flux and rejection rate of the dye solution by the CaAlg hydrogel membrane rehydrated after 40 min of drying, under different operating pressures. It can be seen from Figure 4(a) and (b) that with the increase of operating pressure, the water permeation flux of the membrane gradually increases. This is because the pressure difference is the main driving force for water to pass through the membrane, and the increase of pressure can accelerate the migration rate of water molecules. But the rejection rate remains basically stable, and the rejection rate of dyes is maintained above 80%, indicating that the pore size structure of the CaAlg hydrogel membrane is stable, and it can achieve efficient dye rejection within a certain pressure range (0.05~0.20 MPa), and the pressure change has little effect on the rejection effect.

When the operating pressure reaches 0.15 MPa, the water permeation flux reaches 24 $L \cdot m^{-2} \cdot h^{-1}$, and the rejection rate is stable above 85%. Comprehensively considering the separation efficiency and energy consumption, the appropriate operating pressure is determined to be 0.15 MPa.

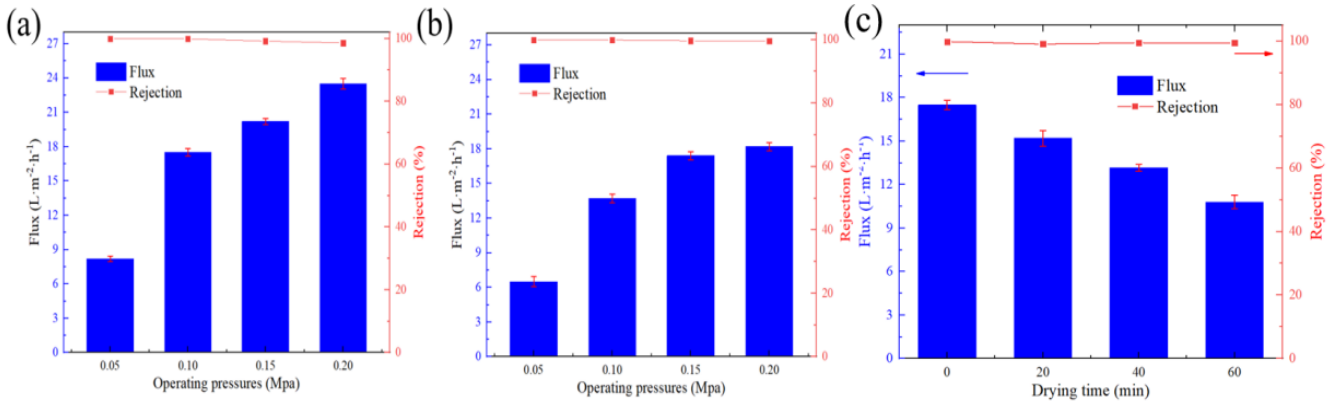

Figure 4. (a) Membrane flux and rejection performance corresponding to different operating pressures under undried condition; (b) Membrane flux and rejection performance corresponding to different operating pressures under the condition of 60 min drying; (c) Membrane flux and rejection performance under different drying times

3.5. Effect of Drying Time on the Membrane Separation Performance

Figure 4(c) shows the change curves of water permeation flux and rejection rate of CaAlg hydrogel membranes under different drying times, with the operating pressure of 0.15 MPa and dye concentration of 50 ppm. It can be seen from the figure that the undried membrane has a high water permeation

flux but a low rejection rate (about 70%). This is because the network structure of the membrane is loose, and part of the dye molecules can leak through the pores.

With the extension of drying time, the water permeation flux gradually decreases, and the rejection rate gradually increases. When the drying time is 40 min, the rejection rate reaches the maximum value (about 88%), and the water permeation flux is maintained at 21 $L \cdot m^{-2} \cdot h^{-1}$, achieving the balance between flux and rejection rate. When the drying time is further extended to 60 min, the water permeation flux further decreases, the rejection rate increases slightly, but the increase range is small, and the membrane appears embrittled, which is not conducive to practical application.

This is because too long drying time will lead to excessive shrinkage of the membrane pore size. Although it improves the rejection rate, it reduces the water permeation flux, and at the same time affects the mechanical toughness of the membrane. Therefore, 40 min is the optimal drying time.

3.6. Effect of Dye Concentration on the Membrane Separation Performance

Figure 5 shows the change curves of water permeation flux and rejection rate of the rehydrated CaAlg hydrogel membrane after 40 min of drying, under different dye concentrations. It can be seen from the figure that with the increase of dye concentration, the water permeation flux of the membrane gradually decreases. This is because dye molecules are adsorbed and deposited on the membrane surface, forming a fouling layer, which hinders the permeation of water molecules.

But the rejection rate remains basically stable, and the rejection rate for different dyes is maintained above 85%. Even when the dye concentration increases to 80 ppm, the rejection rate still has no obvious decrease, indicating that the CaAlg hydrogel membrane has good rejection ability for dyes of different concentrations, and is suitable for the working conditions of large fluctuation of dye concentration in dyeing wastewater.

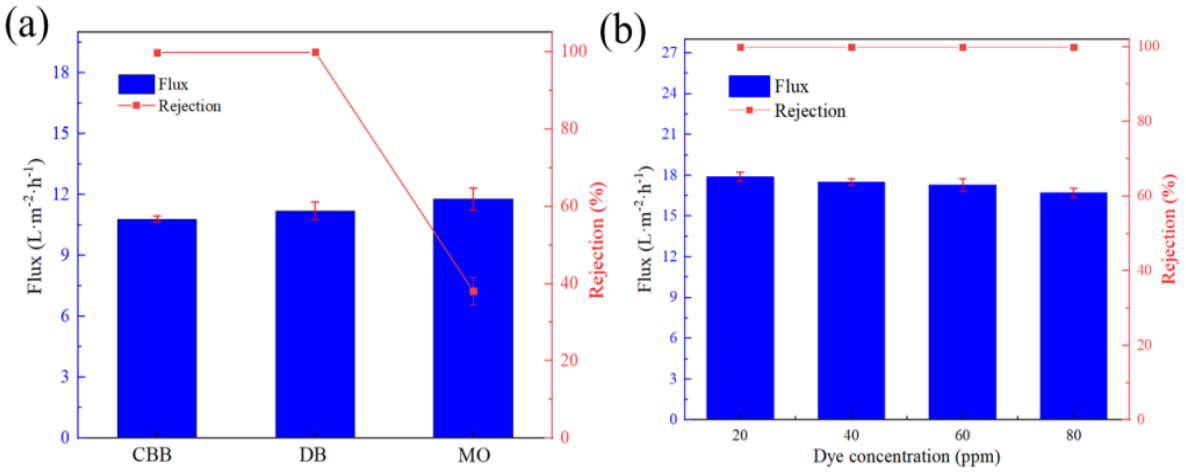

Figure 5. Change curves of water permeation flux and rejection rate of CaAlg hydrogel membrane after 40 min drying and rehydration under different dye concentrations

3.7. Dye/Salt Separation Performance of the Membrane

Figure 6 shows the separation performance curves of CaAlg hydrogel membrane for different dyes and NaCl. It can be seen from the figure that the rejection rate of the membrane for the three dyes DB, MO and CBB all reached above 80%, while the rejection rate for NaCl was lower than 10%, and the separation factor was greater than 90, indicating that the CaAlg hydrogel membrane has good dye/salt separation ability.

This is because the pore size of the CaAlg hydrogel membrane is controllable, which can physically intercept macromolecular dyes. At the same time, the carboxyl groups (-COO-) on the membrane surface undergo electrostatic adsorption with dye molecules, further improving the rejection effect. While NaCl is a small-molecule electrolyte, which can pass through the membrane pores smoothly, achieving the dual purpose of dye enrichment and salt recovery, and adapting to the treatment requirements of high-salt and high-chroma dyeing wastewater.

Compared with the undried CaAlg membrane, the water flux of the CaAlg hydrogel membrane after 60 min of drying decreased slightly, but still maintained a stable level of 8.5 $L \cdot m^{-2} \cdot h^{-1}$, and different dye molecules had little effect on the membrane flux. This is mainly due to the excellent hydrophilicity of the CaAlg material itself. At the same time, the rejection rate of the dried membrane for NaCl still remained at about 10%, and the rejection rate for CBB and DB dyes remained above 95%, indicating that the CaAlg filtration membrane after 60 min of drying also has excellent dye/salt separation performance under low-salt conditions, and can adapt to the treatment requirements of high-salt dyeing wastewater.

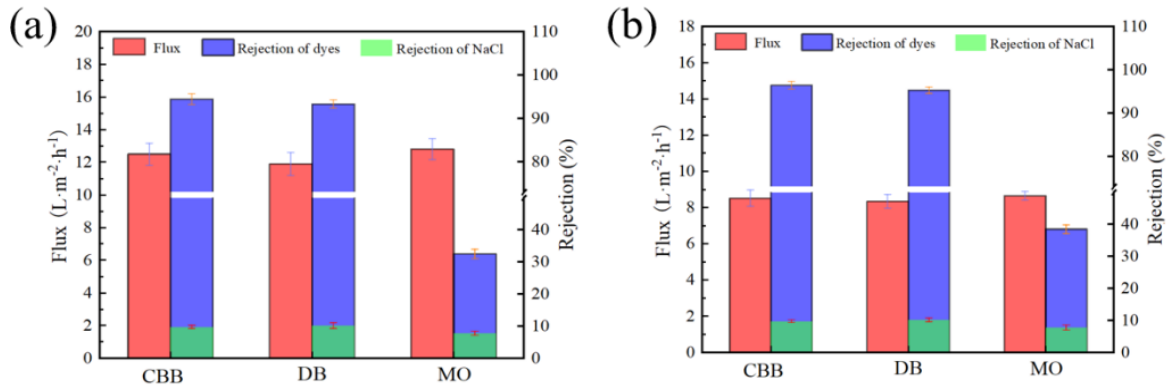

Figure 6. Separation performance curves of CaAlg hydrogel membrane for different dyes and NaCl; (a) Separation performance of undried CaAlg membrane; (b) Separation performance of dried CaAlg membrane

Figure 7 shows the effect of different dye concentrations on the separation performance of the dried CaAlg membrane. As shown in the figure, the dye concentration has little effect on the separation performance of the dried CaAlg hydrogel membrane overall. With the increase of dye concentration, the water flux changes insignificantly (~8.5 $L \cdot m^{-2} \cdot h^{-1}$), while the rejection rate increases slightly (>95%). Experiments demonstrate that the dried CaAlg membrane exhibits excellent separation performance for dyes and salts at low salt concentrations.

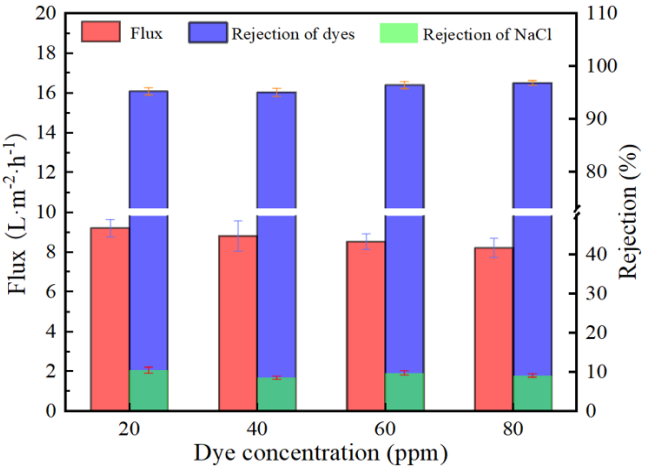

Figure 7. Effect of different dye concentrations on the separation performance of the dried CaAlg membrane

4. Conclusion

In this study, calcium alginate (CaAlg) hydrogel membranes were modified via vacuum drying-rehydration, and the effects of drying time on their structure, mechanical and separation properties were systematically investigated. Main conclusions:

(1) CaAlg filtration membranes were prepared by ionic crosslinking. FT-IR confirmed effective crosslinking between Ca^{2+} and alginate groups; TG-DTG showed CaAlg membranes had better thermal stability than NaAlg, meeting dyeing wastewater treatment temperature requirements.

(2) Vacuum drying-rehydration improved CaAlg membranes' mechanical strength and anti-swelling ability, with optimal drying time of 40 min. Under this condition, rehydrated membrane tensile strength was 1.60 MPa (≈45.5% higher than undried) with good toughness retained.

(3) Under optimized conditions (0.15 MPa, 40 min drying, 50 ppm dye), the optimized CaAlg membrane achieved >85% rejection for three dyes, stable flux of 21 $L \cdot m^{-2} \cdot h^{-1}$, and NaCl rejection <10%, enabling dye enrichment and salt recovery for high-salinity dyeing wastewater.

This study modified CaAlg membranes via vacuum drying-rehydration, solving the insufficient mechanical strength bottleneck of pure CaAlg membranes while maintaining excellent separation performance, and supporting their industrial application in advanced dyeing wastewater treatment.

References

[1] Tummino M L, Nisticò R, Riedo C, Fabbri D, Cerruti M, Magnacca G. Waste Cleaning Waste: Combining Alginate with Biowaste-Derived Substances in Hydrogels and Films for Water Clean-up [J]. Chemistry - A European Journal, 2021, 27(42): 660-668.

[2] Guo J, Zhang Q, Cai Z, Zhao K. Preparation and dye filtration property of electrospun polyhydroxybutyrate-calcium alginate/carbon nanotubes composite nanofibrous filtration membrane [J]. Separation and Purification Technology, 2016, 161: 69-79.

[3] Radoor S, Kandel D R, Chang S, Karayil J, Lee J. Carrageenan/calcium alginate composite hydrogel filtration membranes for efficient cationic dye separation [J]. International Journal of Biological Macromolecules, 2024, 270: 132309.

[4] Wang X, Qin W, Wang L, Zhao K, Wang H, Liu H, Wei J. Desalination of dye utilizing carboxylated TiO_2/calcium alginate hydrogel nanofiltration membrane with high salt permeation [J]. Separation and Purification Technology, 2020, 253: 117564.

[5] Yi K, Fan Z, Tang J, Chen A, Shao J, Peng L, Zeng Q, Luo S. The elucidation of surrounding alginate gels on the pollutants degradation by entrapped nanoscale zero-valent iron [J]. Colloids and Surfaces B: Biointerfaces, 2019, 181: 869-876.

[6] Xu L, Zhao K, Miao J, Yang Z, Li Z, Zhao L, Su H, Lin L, Hu Y. High-strength and anti-bacterial BSA/carboxymethyl chitosan/silver nanoparticles/calcium alginate composite hydrogel membrane for efficient dye/salt separation [J]. International Journal of Biological Macromolecules, 2021, 191: 1086-1095.

[7] Wang F, Zhang H, Sun Y, Wang S, Zhang L, Wu A, Zhang Y. Superhydrophilic quaternized calcium alginate based aerogel membrane for oil-water separation and removal of bacteria and dyes [J]. International Journal of Biological Macromolecules, 2023, 225: 1144-1154.

[8] Zhao Y, Liu X, Qi M, Bai T, Zhao K, Zhang X. Removal of Dyes and Cd2+ in Water by Kaolin/Calcium Alginate Filtration Membrane [J]. Coatings, 2019, 9(4): 218.

[9] Zhao K, Zhang X, Wei J, Li J, Zhou X, Liu D, Liu Z, Li J. Calcium alginate hydrogel filtration membrane with excellent

anti-fouling property and controlled separation performance [J]. Journal of Membrane Science, 2015, 492: 537-546.

[10] Mokhena T C, Mochane M J, Mtibe A, John M J, Sadiku E R, Sefadi J S. Electrospun Alginate Nanofibers Toward Various Applications: A Review [J]. Materials, 2020, 13(4): 934.

[11] Ji D, Park J M, Oh M S, Nguyen T L, Shin H, Kim J S, Kim D, Park H S, Kim J. Superstrong, superstiff, and conductive alginate hydrogels [J]. Nature Communications, 2022, 13: 3019.

[12] Ji D, Nguyen T L, Kim J. Bioinspired Structural Composite Hydrogels with a Combination of High Strength, Stiffness, and Toughness [J]. Advanced Functional Materials, 2021, 31(28): 2101095.

[13] Leon-Cecilla A, Vazquez-Perez F J, Gila-Vilchez C, de Cienfuegos L A, Lopez-Lopez M T. Alginate Hydrogels Reinforced by Dehydration under Stress—Application to a Soft Magnetic Actuator [J]. Gels, 2023, 9(1): 39.

[14] Zhao X, Xia Y, Zhang X, Lin X, Wang L. Design of mechanically strong and tough alginate hydrogels based on a soft-brittle transition [J]. International Journal of Biological Macromolecules, 2019, 139: 850-857.

[15] Yang Q, Hu Z, Rogers J A. Functional Hydrogel Interface Materials for Advanced Bioelectronic Devices [J]. Accounts of Materials Research, 2021, 2(11): 1010-1023.

[16] Chui C, Bonilla-Brunner A, Seifert J, Contera S, Ye H. Atomic Force Microscopy-indentation demonstrates that Alginate Beads are mechanically stable under Cell Culture Conditions [J]. Journal of the Mechanical Behavior of Biomedical Materials, 2019, 93: 61-69.

[17] Wang L, Zhang H J, Liu X, Liu Y, Zhu X, Liu X, You X. A Physically Cross-Linked Sodium Alginate–Gelatin Hydrogel with High Mechanical Strength [J]. ACS Applied Polymer Materials, 2021, 3(6): 3197-3205.

[18] Calija B, Cekić N, Savić S, Daniels R, Marković B, Milić J. pH-sensitive microparticles for oral drug delivery based on alginate/oligochitosan/Eudragit® L100-55 “sandwich” polyelectrolyte complex [J]. Colloids and Surfaces B: Biointerfaces, 2013, 110: 395-402.

[19] Xu L, Xie W, Zhao K, Shi W, Jiang J, Lin L. Chlorine-resistance, reswelling after drying and molecule/ions separation properties of carboxyl multi-walled carbon nanotubes/calcium alginate composite hydrogel membrane [J]. Composites Communications, 2022, 34: 101258.